Published in final edited form as:
J Cardiovasc Electrophysiol. 2009 September ; 20(9): 1048–1054. doi:10.1111/j.1540-8167.2009.01475.x.

Synergistic effects of Inward Rectifier (I_{K1}) and Pacemaker (I_f) Currents on the Induction of Bioengineered Cardiac Automaticity

Hung-Fat Tse, MD, PhD[1,2], **Chung-Wah Siu, MBBS**[1,4,*], **Yau-Chi Chan, MPhil**[1,*], **Yee-Man Lau, PhD**[1,*], **Chu-Pak Lau, MD**[1], and **Ronald A. Li, PhD**[1,5]

[1]Cardiology Division, Department of Medicine, University of Hong Kong

[2]Stem Cell & Regenerative Medicine Program, Research Centre of Heart, Brain, Hormone and Healthy Aging, Li Ka Shing Faculty of Medicine, University of Hong Kong

[3]Stem Cell Program, University of California, Davis, CA.

[4]Department of Cell Biology and Human Anatomy, University of California, Davis, CA.

[5]Institute of Pediatric Regenerative Medicine, Shriners Hospital for Children of North America, Sacramento, CA.

Abstract

Introduction—Normal heart rhythms originate in the sinoatrial node. HCN-encoded funny current (I_f) and the Kir2-encoded inward rectifier (I_{K1}) counteract each other by respectively oscillating and stabilizing the negative resting membrane potential, controlling action potential firing. Therefore, I_{K1} suppression and I_f overexpression have been independently exploited to convert cardiomyocytes (CMs) into AP-firing bioartificial pacemakers. Although the two strategies have been largely assumed synergistic, their complementarity has not been investigated.

Methods and Results—We explored the inter-relationships of automaticity, I_f and I_{K1} by transducing single left ventricular (LV) CMs isolated from guinea pig hearts with the recombinant adenoviruses Ad-CMV-GFP-IRES-HCN1-ΔΔΔ and/or Ad-CGI-Kir2.1 to mediate their current densities via whole-cell patch clamp technique at 37°C. Results showed that Ad-CGI-HCN1-ΔΔΔ- but not Ad-CGI-Kir2.1-transduction induced automaticity (181.1±13.1 bpm). Interestingly, Ad-CGI-HCN1-ΔΔΔ/Ad-CGI-Kir2.1 cotransduction significantly promoted the induced firing frequency (320.0±15.8 bpm; $p<0.05$). Correlation analysis revealed that the firing frequency, phase 4 slope and APD_{90} of AP-firing LV CMs were correlated to I_f ($R^2>0.7$) only when $-2>I_{K1}>-4$ pA/pF but not to I_{K1} over the entire I_f ranges examined ($0.02<R^2<0.4$). Unlike I_f, I_{K1} displayed correlation to neither the phase 4 slope ($R^2=0.02$) nor phase 4 length ($R^2=0.04$) when $-2>I_f>-4$ pA/pF. As anticipated, however, APD_{90} was correlated to I_{K1} ($R^2=0.4$).

Conclusion—We conclude that an optimal level of I_{K1} maintains a voltage range for I_f to operate most effectively during a dynamic cardiac cycle.

Keywords

I_f; I_{K1}; bioartificial pacemaker; automaticity; synergism

Address for correspondence: Hung-Fat Tse, MD, PhD, Cardiology Division, Department of Medicine, The University of Hong Kong, Rm 1928, Block K, Queen Mary Hospital, Hong Kong. Tel: 852-28553598 Fax: 852-28186304. Email: hftse@hkucc.hku.hk..
*Drs. Siu and Chan contributed equally to this work.

Introduction

Normal heart rhythms originate in the sinoatrial node (SAN), a specialized cardiac tissue consisting of only a few thousand pacemaker cells. Funny current (I_f), encoded by the hyperpolarization-activated cyclic nucleotide-modulated (HCN) channel gene family plays a pivotal role in the generation of cardiac rhythms in nodal pacemaker cells. It serves as an intrinsic oscillator that drives diastolic depolarization to the action potential (AP) threshold after each excitation cycle.1-5 By contrast, the Kir2-encoded inwardly rectifying potassium current (I_{K1}) has the dual function of stabilizing a negative resting membrane potential (RMP) and facilitating repolarization.6 Indeed, the robust expression of I_f and the lack of I_{K1} are a signature of rhythmically-firing nodal pacemaker cells.3,7 Conversely, I_{K1} but not I_f is robustly expressed in silent-yet-excitable adult atrial and ventricular cardiomyocytes (CMs).8,9 As such, the approaches of I_{K1} suppression10,11 and I_f over-expression,4,5,12-14 have been independently and, most commonly, exploited to convert normally quiescent CMs into spontaneously AP-firing cells as bioartificial pacemakers. Although the two strategies appear to be conceptually synergistic, their complementarity has not been experimentally investigated. Indeed, single-sided reproduction of either the I_f or I_{K1} profile of nodal cells in the atrial or ventricular CMs may not be optimal for inducing and modulating automaticity. 15 Atrial and ventricular CMs have repertoires of ionic currents that are different from those of nodal pacemaker cells. Since I_f is activated by hyperpolarization and deactivated by depolarization, here we hypothesize that I_{K1}, a presumptive opponent of I_f, synergistically enhances I_f by maintaining the voltage changes within a range where HCN channels can most effectively operate during a dynamic cardiac cycle.

Methods

Molecular biology

PCR-based mutagenesis of mouse HCN1 (generously provided by Dr. Steve Segalbaum, Columbia University) of the bicistronic adenovirus shuttle vector pAdCMV-GFP-IRES (or pAdCGI) was performed with overlapping oligos as described previously.16,17 The internal ribosomal entry site (IRES) allows the simultaneous translation of 2 transgenes, green fluorescence protein (GFP) and an engineered-HCN1 construct, with a single transcript. HCN1 was chosen since its structure-function properties have been extensively investigated in our previous studies.15-25 Adenoviruses were generated by Cre-lox recombination of purified ψ5 viral DNA and shuttle vector DNA using Cre4 cells.26 The recombinant products were plaque purified, amplified, and purified again by CsCl gradients, yielding concentrations on the order of 10^{10} plaque-forming units (PFU) ml^{-1}.

Adenovirus-mediated gene transfer and isolation of LV CMs

Adult female guinea pigs (~250-300g) were euthanized by intraperitoneal injection of pentobarbital (80mg/kg). The hearts were quickly excised, followed by perfusion with enzymatic solutions using a customized Langendorff apparatus. Left ventricular (LV) CMs were plated at 5×10^5 per laminin-coated glass coverslip in medium containing: 5 mM carnitine, 5 mM creatine, 5 mM taurine, 100 μg ml^{-1} penicillin-streptomycin and 10% fetal bovine serum in Medium 199 (Sigma-Aldrich Corp., St. Louis, MO, USA) in a 37°C incubator with 5% CO_2 for 2 hrs. For transduction, LV CMs were incubated for 1 hour in serum-free medium containing adenoviral particles at a concentration of ~2×10^9 PFU. A transduction efficiency of ~70-80% could typically be achieved with this protocol. Such an *in vitro* system of adult guinea pig LV CMs has been previously used by both us 27 and others.28

Electrophysiology and data analysis

Electrical recordings were performed using the whole-cell patch-clamp technique at 37°C (HEKA Instruments Inc. Southboro, MA, USA). Successfully transduced cells were selected based on their epifluorescence at 488/530 nm (excitation/emission). Patch pipettes were prepared from 1.5 mm thin-walled borosilicate glass tubes using a Sutter micropipette puller P-97 and had typical resistances of 3-5 MΩ when filled with an internal solution containing (mM): 110 K^+ aspartate, 20 KCl, 1 $MgCl_2$, 0.1 Na-GTP, 5 Mg-ATP, 5 Na_2-phosphocreatine, 1 EGTA, 10 HEPES, pH adjusted to 7.3 with KOH. The external Tyrode's bath solution was composed of (mM): 140 NaCl, 5 KCl, 1 $MgCl_2$, 1 $CaCl_2$, 10 Glucose, 10 HEPES, pH adjusted to 7.4 with NaOH. Cell capacitance was measured by using the internal circuit for capacitance-current compensation, in which both cell capacitance and series resistance were compensated. Voltage-and current-clamp recordings were simultaneously performed on the same cells at 37°C within 24 to 36 hours after transduction. *Absolutely* no automaticity was detected from cultured control LV CMs recorded over the same period.

To elicit inward currents, cells were held at -30mV and pulsed from 0mV to -140mV with 10mV increments for 3 seconds. I_f was defined as 1mM Ba^{2+}-insensitive, time-dependent currents. For recording action potentials, cells were held at 0pA without (for electrically-active cells) or with a stimulation of 0.1-1nA for 5ms to elicit a response. The steady-state current-voltage (*I-V*) relationship of I_f was determined by plotting the currents measured at the end of the 3-second test pulses of the above-mentioned protocol against the test potentials in the presence of 1mM $BaCl_2$. Data were not corrected for the junction potential.

Statistical analysis

Correlation analysis was performed by linear regression. The larger the value of R^2, the better correlation of the two parameters in comparison. . All data reported were means ± S.E.M. with $P<0.05$ indicating statistical significance as determined using an unpaired Student's *t* test.

Results

Adenovirus-mediated overexpression of I_f and/or I_{K1} in adult LV CMs

For I_f and/or I_{K1} overexpression, we generated the recombinant adenoviruses Ad-CGI-HCN1-ΔΔΔ and Ad-CGI-Kir2.1 that mediate ectopic expression of HCN1-ΔΔΔ and Kir2.1 channels, respectively. The engineered HCN1 construct, HCN1-ΔΔΔ whose S3-S4 linker has been shortened by deleting residues 235-237 to favor channel opening,[16,17,23] was chosen to best mimic native heteromultimeric I_f in adult LV CMs without having to consider poorly defined factors such as accessory subunits and cellular context as we previously described.[4,5] Figure 1A shows that all control LV CMs were electrically quiescent but capable of generating a single AP upon stimulation by a depolarizing current pulse (800 pA for 2 to 5 ms; n=17). Consistent with our previous results,[4,5] robust I_{K1} (-32.1±1.2 pA/pF at -140mV) but no detectable I_f (-2.5±1.0 pA/pF at -140mV) could be recorded from the same control LV CMs.

We next studied the effect of transducing LV CMs with Ad-CGI-Kir2.1 (Figure 1B), Ad-CGI-HCN1-ΔΔΔ (Figure 1C) and both (Figure 1D). For Ad-CGI-Kir2.1-transduced LV CMs, there was a significant increase in I_{K1} relative to control (-101.2±3.2 pA/pF at -140 mV; $p<0.05$), but I_f was still absent (-1.8±1.1 pA/pF at -140 mV; $p<0.05$). By contrast, I_{K1} in Ad-CGI-HCN1-ΔΔΔ-trasnduced LV CMs (-34.8±5.5 pA/pF at -140 mV; n=5) was not different from control ($p>0.05$), but hyperpolarization-activated time-dependent I_f could be readily recorded (-28.5±3.9 pA/pF at -140 mV; $p<0.05$). For LV CMs simultaneously cotransduced by Ad-CGI-HCN1-ΔΔΔ and Ad-CGI-Kir2.1-WT, both I_{K1} (-46.6±5.5 pA/pF

at -140 mV; n=9) and I_f (-40.7±6.4 pA/pF at -140 mV; n=9) were substantially expressed. The corresponding current-voltage relationships are given (Figure 1E-H).

Coexpression of I_f and I_{K1} promoted induced automaticity

To directly probe the functional consequences of overexpressing I_f or I_{K1} alone or both in the AP waveform, we subjected the same cells presented above to current-clamp recordings. While Ad-CGI-Kir2.1-transduction significantly hyperpolarized the RMP (-69.7±0.7 mV vs. -66.0±0.7 mV of WT; $p<0.05$) (Figure 2A) and shortened the duration of AP elicited upon a depolarizing current stimulus (by ~65%, n=7; $p<0.05$) (Figure 2B and Table 1), Ad-CGI-HCN1-ΔΔΔ uniquely induced ventricular automaticity (n=10), even without stimulation, with a firing rate of 181.1±13.1 bpm, a relatively depolarized maximum diastolic potential (MDP = -55.8±1.8 mV) and phase-4 depolarization (180±20 mV/s), consistent with what we recently reported.4,5 Spontaneous APs were never observed in either control or Ad-CGI-Kir2.1-transduced LV CMs. Interestingly, simultaneous overexpression of I_f and I_{K1} significantly promoted the induced automaticity by increasing the AP-firing frequency by ~1.8-fold to 320.0±15.8 bpm (n=9; $p<0.05$) (Figure 2C). Relative to single Ad-CGI-HCN1-ΔΔΔ transduction, cotransduced LV CMs had significantly ($p<0.05$) hyperpolarized MDP (-57.1±0.9 mV, Figure 2A), hastened phase 4 depolarization (280±16 mV/s, Figure 2D) and shortened APD_{90} (by 56% to 97.3±7.9 ms from 199.5±8.7 ms). All these AP parameters as well as cycle length and APD_{50} of control and transduced LV CMs are summarized in Table 1.

As I_{K1} plays important roles in setting the resting membrane potential and in influencing the final phase of repolarization, the accelerated firing rate in cotransduced LV CMs may be a consequence of a greater magnitude of I_f due to the more negative membrane potential, or of a shorter AP duration due to a more rapid repolarization, or both. In order to dissect these I_{K1}-dependent effects contributing to the accelerated firing rate, we measured firing rate, action potential duration, phase-4 slope and phase-4 duration of automatic cotransduced LV CMs by pharmacological blockade of I_{K1} with external Ba^{2+} at concentration of 0.1 mM and 0.3 mM. At baseline, the cycle length was 257.8±6.0 ms, i.e., 233.9±5.4 bpm with APD_{90} of 94.8±1.0 ms and phase-4 length of 68.7±2.7 ms. As expected, external application of Ba^{2+}(0.1 mM) shifted the maximal diastolic potential from -45.9±0.1 mV to -29.1±0.3 mV, which was associated with a reduction of firing rate for 26.8%. Although the APD_{90} was lengthened by 58 ms, i.e., 61.2% increment, the phase-4 duration were prolonged by67.4 ms (98.2%) due to the flattening of the phase-4 slope by 51.2%. However, further increase in external Ba^{2+} concentration to 0.3 mM resulted in a complete abortion of automaticity. These data suggests that I_{K1} accelerates the firing rate of I_f induced automaticity by enhancing the phase-4 slope as well as shortening AP duration.

Inter-relationships between I_{K1}, I_f and automaticity

For shedding mechanistic insights, we next investigated the intricate inter-relationships among I_{K1}, I_f and induced automaticity. To obtain a more global and accurate view, we plotted the various biophysical parameters recorded from *all* of control, singly- and doubly-transduced LV CMs to generate broader ranges for correlation analyses (i.e., the different experimental groups were included on the same plots in different symbols, but the entire data sets were fitted to liner regression). In spontaneously AP-firing cells, the frequency did not depend on the amplitude of I_f at -60 mV ($I_{f,\ -60mV}$) when I_{K1} at -60 mV ($I_{K1,\ -60mV}$) was ≥-2 pA/pF (R^2=0.03; Figure 4A, solid squares). However, the induced firing rate displayed a strong positive correlation to $I_{f,\ -60mV}$ when $-2>I_{K1,\ -60mV}>-4$ pA/pF (R^2=0.8; Figure 4A, open circles). Such a positive correlation diminished (to R^2=0.3) as $I_{K1,\ -60mV}$ increased to ≤ -4 pA/pF (Figure 4A, solid triangle). In stark contrast to I_f, the induced automaticity did not

depend on $I_{K1, -60mV}$ when $I_{f, -60mV}$ was similarly fixed (i.e. $I_{f, -60mV} \leq 2pA/pF$, $-2 < I_{f, -60mV} \leq 4pA/pF$ and $I_{f, -60mV} > 4pA/pF$; Figure 4B).

To further dissect the inter-relationship, we similarly plotted the Phase 4 slope, Phase 4 length, and APD_{90} against $I_{f, -60mV}$ with fixed ranges of $I_{K1, -60mV}$. Similar to the firing frequency, all these AP parameters were also correlated to $I_{f, -60mV}$ only when $-2 > I_{K1} > -4$ pA/pF. Figure 5A shows that steeper Phase 4 slopes could be attained with higher I_f densities ($R^2=0.7$). Both the Phase 4 length (Figure 5C; $R^2=0.6$) and APD_{90} (Figure 5E; $R^2=0.7$) were negatively correlated to $I_{f, -60mV}$. Unlike $I_{f, -60mV}$, $I_{K1, -60mV}$ displayed correlation to neither the Phase 4 slope (to $R^2=0.02$) nor Phase 4 length (to $R^2=0.04$) when $-2 > I_{f, -60mV} > -4$ pA/pF (Figures 5B & D). As anticipated, however, APD_{90} was correlated to $I_{K1, -60mV}$ (to $R^2=0.4$; Figure 5F).

Isoproterenol accelerates firing rate of Ad-CGI-HCN1-ΔΔΔ transduced LV CMs

To test the functionality of automatic Ad-CGI-HCN1-ΔΔΔ-transduced LV CMs as a pacemaker, we investigated their response to adrenergic stimulation by superfusion of 1 μM isoproterenol for 5 minutes. The cycle length reduced from 377±8.7 to 318±10.1 ms ($p=0.001$; n=3) representing 18% increase in the firing rate (Figure 6). This is largely due to the increase of phase-4 slope (166±9.5 mV/s to 265±11.9 mV/s, $p=0.003$), while the APD_{90}, maximal diastolic potential and take-off potential were largely unchanged after isoproterenol treatment.

Discussion

In recent years, efforts to generate bioartificial pacemakers as potential alternatives or supplements to electronic devices for treating cardiac rhythm disorders have been pursued. Experimentally, the one-sided approaches of maximizing I_f 4,12 or minimizing its "antagonizing" I_{K1} 10,29 to convert nonpacing CMs to spontaneously firing pacemaker cells have been investigated. Our previous *in silico* and *in vivo* HCN-gene-transfer experiments of LV CMs demonstrate that both I_f and I_{K1} play critical roles in the induction of automaticity 4, 5, 21. While the two strategies appear to be conceptually synergistic, their complementarity has not been investigated. Indeed, although the primary functions of I_{K1} and I_f have been largely presumed to antagonize each other, our present study provides novel experimental supports that they do not necessarily counter-balance each other. Firstly, adenovirus-mediated expression of I_f (or I_{K1}) in LV CMs did not alter I_{K1} (or I_f). These observations suggest that the two "opposing" currents do not undergo compensatory electrophysiological changes against each other when their relative expression is altered. As such, the resultant AP phenotypes can be principally attributed to the changes of either I_f or I_{K1} alone. Secondly, simultaneous overexpression of I_f and I_{K1} in LV CMs generates the highest oscillation frequency of automaticity. Correlation analysis to dissect the intricate mechanistic relationships among various I_f, I_{K1} and AP biophysical parameters indicates that, mechanistically, the frequency of induced AP-firing cells was dependent upon I_f when $I_{K1, -60mV}$ was between -2 and -4 pA/pF. However, the induced automaticity did not rely on I_{K1} when $I_{f, -60mV}$ was similarly fixed. Thus, the data were in accordance with the notion that I_{K1} functions only as a binary switch for automaticity without providing a direct means for frequency modulation4,5, and further indicate that the strategies of I_{K1} suppression and I_f overexpression are not necessarily synergistic in conferring automaticity on quiescent cardiac muscles.

While the level of induced automaticity by simultaneous I_f and I_{K1} overpression is tachycardic and, as such, not desirable for bioartificial pacing, the findings have significant implications. Clinically, the implantation site for bioartificial pacemaker needs to be carefully considered because the different extents of innervations and the differential

responses of I_{K1} and I_f to endogenous sympathetic and parasympathetic inputs might significantly alter the I_f/I_{K1} ratio from the original level, thereby leading to unanticipated tachyarrhythmias. Mechanistically, it is clear that the I_f/I_{K1} ratio is a more effective parameter to engineer for automaticity induction to generate bioartificial pacemakers than manipulating either I_f or I_{K1} *per se*. As a complex and heterogeneous tissue, the SAN displays gradual changes in phenotypic properties such as ionic current densities, potential profile and gap junction expression from the center (dominant pacemaker range) to the periphery (subsidiary pacemaker range) of the nodal cells.30 While the maximum diastolic potential is more negative, the AP is shorter with faster spontaneous rate in the center than in the periphery, AP is first initiated in the center and then transmitted to the periphery of the SAN.31 Such gradients ensure normal AP propagation in appropriate directions. Our present findings therefore raise the possibility that bioengineered cells that mimic the central and peripheral SA nodal cells showing native AP gradient can be best engineered by targeted firing rate engineering via virus cotransduction to improve the functional efficacy.

Of note, the current study has certain limitations. The choice of a gate-engineered version of HCN1 instead of wild-type HCN4 (the predominant HCN in genuine biological pacemakers) appears nonphysiological. However, this is because overexpression of wild-type HCN4 alone does not suffice to cause automaticity in adult LV CMs, probably due to the vast differences in ion channel panoplies as well as certain contentious β-subunits between sinoatrial pacemaker cells and normally quiescent adult LV CMs.13 Consequently, the use of this gate-engineered version of HCN1 may compensate for any context-dependent gating effects such as other modifying subunits and factors that may be present in SA nodal cells but not CMs. Second, the expression of I_f and I_{K1} in the present work were sporadic in nature due to the available transduced method, which may render a large variation in certain physiological measurement such as APD.

Conclusion

Based on the present results, we conclude that the induction of automaticity in LV CMs requires a fine balance of I_{K1} and I_f. Indeed, I_{K1} synergistically interacts with I_f by maintaining the voltage changes within a range where HCN channels can most effectively operate during a dynamic cardiac cycle.

Acknowledgments

This work was supported by grants from the NIH (R01 HL72857 to R.A.Li), the Stem Cell Program of the University of California (to R.A.Li), and the Hong Kong Research Grant Council (HKU 7459/04M to C.P.Lau, H.F.Tse, and R.A.Li). C.W.Siu was supported by a postdoctoral fellowship award from the Croucher Foundation.

References

1. DiFrancesco D. Pacemaker mechanisms in cardiac tissue. Annu Rev Physiol. 1993; 55:455–72. [PubMed: 7682045]
2. Irisawa H, Brown HF, Giles W. Cardiac pacemaking in the sinoatrial node. Physiol Rev. 1993; 73:197–227. [PubMed: 8380502]
3. Siu CW, Lieu DK, Li RA. HCN-encoded pacemaker channels: from physiology and biophysics to bioengineering. J Membr Biol. 2006; 214(3):115–22. [PubMed: 17558529]
4. Tse HF, Xue T, Lau CP, Siu CW, Wang K, Zhang QY, Tomaselli GF, Akar FG, Li RA. Bioartificial sinus node constructed via in vivo gene transfer of an engineered pacemaker HCN Channel reduces the dependence on electronic pacemaker in a sick-sinus syndrome model. Circulation. Sep 5; 2006 114(10):1000–11. [PubMed: 16923751]

5. Xue T, Siu CW, Lieu DK, Lau CP, Tse HF, Li RA. Mechanistic role of I(f) revealed by induction of ventricular automaticity by somatic gene transfer of gating-engineered pacemaker (HCN) channels. Circulation. Apr 10; 2007 115(14):1839–50. [PubMed: 17389267]
6. Dhamoon AS, Jalife J. The inward rectifier current (IK1) controls cardiac excitability and is involved in arrhythmogenesis. Heart Rhythm. Mar; 2005 2(3):316–24. [PubMed: 15851327]
7. Dobrzynski H, Boyett MR, Anderson RH. New insights into pacemaker activity: promoting understanding of sick sinus syndrome. Circulation. Apr 10; 2007 115(14):1921–32. [PubMed: 17420362]
8. Schram G, Pourrier M, Melnyk P, Nattel S. Differential distribution of cardiac ion channel expression as a basis for regional specialization in electrical function. Circ Res. May 17; 2002 90(9):939–50. [PubMed: 12016259]
9. Yu H, Chang F, Cohen IS. Pacemaker current exists in ventricular myocytes. Circ Res. Jan; 1993 72(1):232–6. [PubMed: 7678078]
10. Miake J, Marban E, Nuss HB. Functional role of inward rectifier current in heart probed by Kir2.1 overexpression and dominant-negative suppression. J Clin Invest. May; 2003 111(10):1529–36. [PubMed: 12750402]
11. Milanesi R, Baruscotti M, Gnecchi-Ruscone T, DiFrancesco D. Familial sinus bradycardia associated with a mutation in the cardiac pacemaker channel. N Engl J Med. Jan 12; 2006 354(2): 151–7. [PubMed: 16407510]
12. Bucchi A, Plotnikov AN, Shlapakova I, Danilo P Jr. Kryukova Y, Qu J, Lu Z, Liu H, Pan Z, Potapova I, KenKnight B, Girouard S, Cohen IS, Brink PR, Robinson RB, Rosen MR. Wild-type and mutant HCN channels in a tandem biological-electronic cardiac pacemaker. Circulation. Sep 5; 2006 114(10):992–9. [PubMed: 16923750]
13. Qu J, Barbuti A, Protas L, Santoro B, Cohen IS, Robinson RB. HCN2 overexpression in newborn and adult ventricular myocytes: distinct effects on gating and excitability. Circ Res. Jul 6; 2001 89(1):E8–14. [PubMed: 11440985]
14. Qu J, Plotnikov AN, Danilo P Jr. Shlapakova I, Cohen IS, Robinson RB, Rosen MR. Expression and function of a biological pacemaker in canine heart. Circulation. Mar 4; 2003 107(8):1106–9. [PubMed: 12615786]
15. Lieu DK, Chan YC, Lau CP, Tse HF, Siu CW, Li RA. Overexpression of HCN-encoded pacemaker current silences bioartificial pacemakers. Heart Rhythm. Sep; 2008 5(9):1310–7. [PubMed: 18693074]
16. Lesso H, Li RA. Helical secondary structure of the external S3-S4 linker of pacemaker (HCN) channels revealed by site-dependent perturbations of activation phenotype. J Biol Chem. Jun 20; 2003 278(25):22290–7. [PubMed: 12668666]
17. Tsang SY, Lesso H, Li RA. Critical intra-linker interactions of HCN1-encoded pacemaker channels revealed by interchange of S3-S4 determinants. Biochem Biophys Res Commun. Sep 17; 2004 322(2):652–8. [PubMed: 15325279]
18. Au KW, Siu CW, Lau CP, Tse HF, Li RA. Structural and functional determinants in the S5-P region of HCN-encoded pacemaker channels revealed by cysteine-scanning substitutions. Am J Physiol Cell Physiol. Jan; 2008 294(1):C136–44. [PubMed: 17989208]
19. Azene EM, Xue T, Li RA. Molecular basis of the effect of potassium on heterologously expressed pacemaker (HCN) channels. J Physiol. Mar 1; 2003 547(Pt 2):349–56. [PubMed: 12562911]
20. Azene EM, Sang D, Tsang SY, Li RA. Pore-to-gate coupling of HCN channels revealed by a pore variant that contributes to gating but not permeation. Biochem Biophys Res Commun. Feb 25; 2005 327(4):1131–42. [PubMed: 15652514]
21. Azene EM, Xue T, Marban E, Tomaselli GF, Li RA. Non-equilibrium behavior of HCN channels: insights into the role of HCN channels in native and engineered pacemakers. Cardiovasc Res. Aug 1; 2005 67(2):263–73. [PubMed: 16005302]
22. Henrikson CA, Xue T, Dong P, Sang D, Marban E, Li RA. Identification of a surface charged residue in the S3-S4 linker of the pacemaker (HCN) channel that influences activation gating. J Biol Chem. Apr 18; 2003 278(16):13647–54. [PubMed: 12582169]

23. Tsang SY, Lesso H, Li RA. Dissecting the structural and functional roles of the S3-S4 linker of pacemaker (hyperpolarization-activated cyclic nucleotide-modulated) channels by systematic length alterations. J Biol Chem. Oct 15; 2004 279(42):43752–9. [PubMed: 15299004]
24. Xue T, Marban E, Li RA. Dominant-negative suppression of HCN1- and HCN2-encoded pacemaker currents by an engineered HCN1 construct: insights into structure-function relationships and multimerization. Circ Res. Jun 28; 2002 90(12):1267–73. [PubMed: 12089064]
25. Xue T, Li RA. An external determinant in the S5-P linker of the pacemaker (HCN) channel identified by sulfhydryl modification. J Biol Chem. Nov 29; 2002 277(48):46233–42. [PubMed: 12351622]
26. Hardy S, Kitamura M, Harris-Stansil T, Dai Y, Phipps ML. Construction of adenovirus vectors through Cre-lox recombination. J Virol. Mar; 1997 71(3):1842–9. [PubMed: 9032314]
27. Ennis IL, Li RA, Murphy AM, Marban E, Nuss HB. Dual gene therapy with SERCA1 and Kir2.1 abbreviates excitation without suppressing contractility. J Clin Invest. Feb; 2002 109(3):393–400. [PubMed: 11827999]
28. Li RA, Ennis IL, Tomaselli GF, Marban E. Structural basis of differences in isoform-specific gating and lidocaine block between cardiac and skeletal muscle sodium channels. Mol Pharmacol. Jan; 2002 61(1):136–41. [PubMed: 11752214]
29. Miake J, Marban E, Nuss HB. Biological pacemaker created by gene transfer. Nature. Sep 12; 2002 419(6903):132–3. [PubMed: 12226654]
30. Dobrzynski H, Li J, Tellez J, Greener ID, Nikolski VP, Wright SE, Parson SH, Jones SA, Lancaster MK, Yamamoto M, Honjo H, Takagishi Y, Kodama I, Efimov IR, Billeter R, Boyett MR. Computer three-dimensional reconstruction of the sinoatrial node. Circulation. Feb 22; 2005 111(7):846–54. [PubMed: 15699261]
31. Boyett MR, Honjo H, Kodama I. The sinoatrial node, a heterogeneous pacemaker structure. Cardiovasc Res. Sep; 2000 47(4):658–87. [PubMed: 10974216]

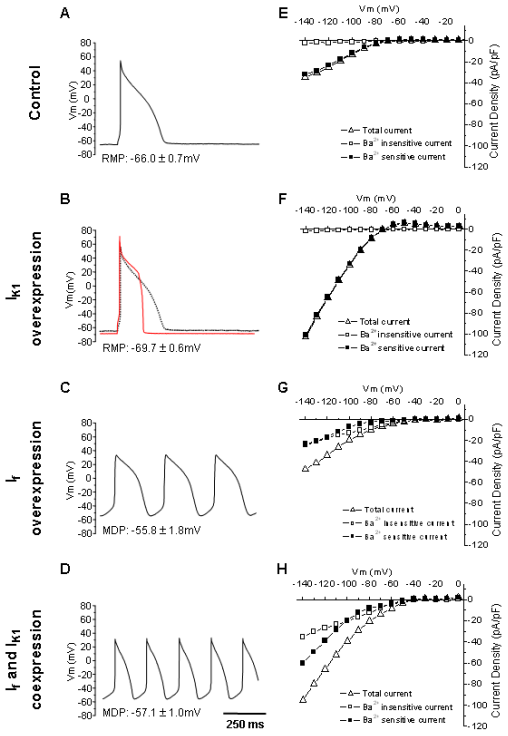

Figure 1.

Representative action potential waveforms and averaged steady-state *I-V* relationships of control **(A, E)**, Ad-CGI-Kir2.1- **(B, F)**, Ad-CGI-HCN1ΔΔΔ- **(C, G)**, as well as Ad-CGI-HCN1ΔΔΔ/Ad-CGI-Kir2.1 **(D, H)**-tranduced LV CMs.

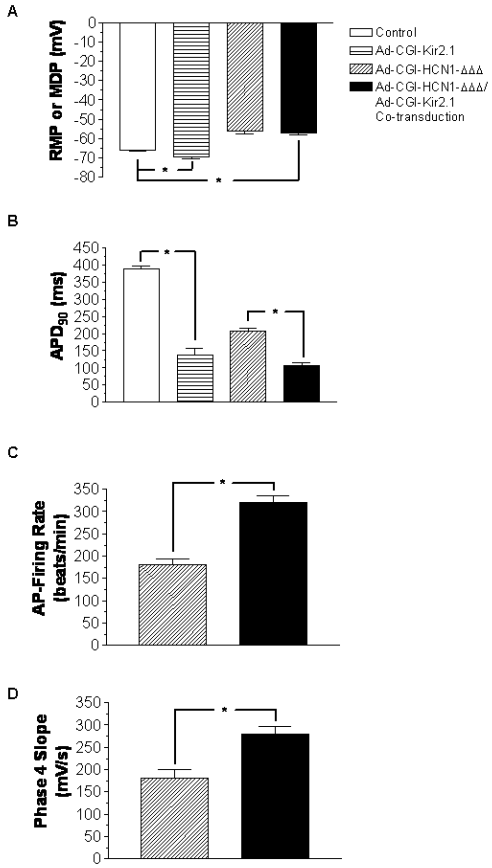

Figure 2.

Bar charts showing **(A)** RMP or MDP; **(B)** APD_{90}; **(C)** beating rate; and **(D)** phase 4 slope of control, Ad-CGI-Kir2.1-transduced, Ad-CGI-HCN1ΔΔΔ-transduced, as well as Ad-CGI-HCN1ΔΔΔ/Ad-CGI-Kir2.1-cotranduced LV CMs. *, $P<0.05$.

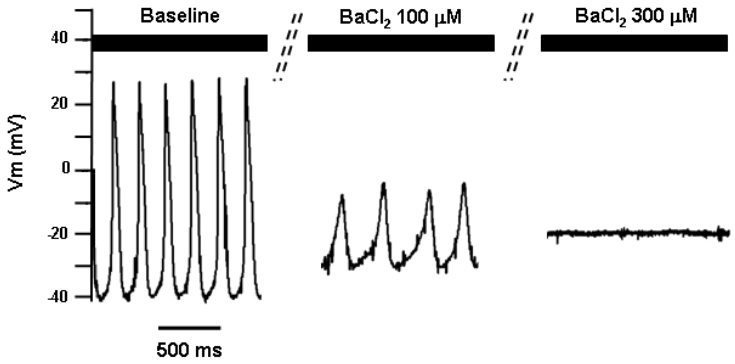

Figure 3.
The effect of external application of Ba^{2+} on the automaticity in Ad-CGI-HCN1ΔΔΔ/Ad-CGI-Kir2.1-cotranduced LV CMs. Representative action potential waveforms at baseline, with 0.1 mM $BaCl_2$, and 0.3 mM $BaCl_2$ are shown, respectively.

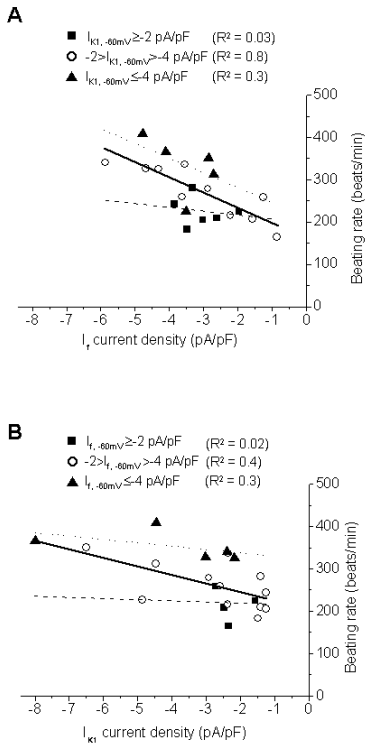

Figure 4.

(A) Correlations between I_f and the frequency of spontaneously AP-firing cells when $I_{K1, -60mV}$ ≥-2 pA/pF (■), -2>$I_{K1, -60mV}$ >-4 pA/pF (○) and $I_{K1, -60mV}$ ≤-4 pA/pF (▲). **(B)** Correlations between I_{K1} and the firing frequency rate when $I_{f, -60mV}$ ≥-2 pA/pF (■),-2>$I_{f, -60mV}$ >-4 pA/pF (○) and $I_{f, -60mV}$ ≤-4 pA/pF (▲).

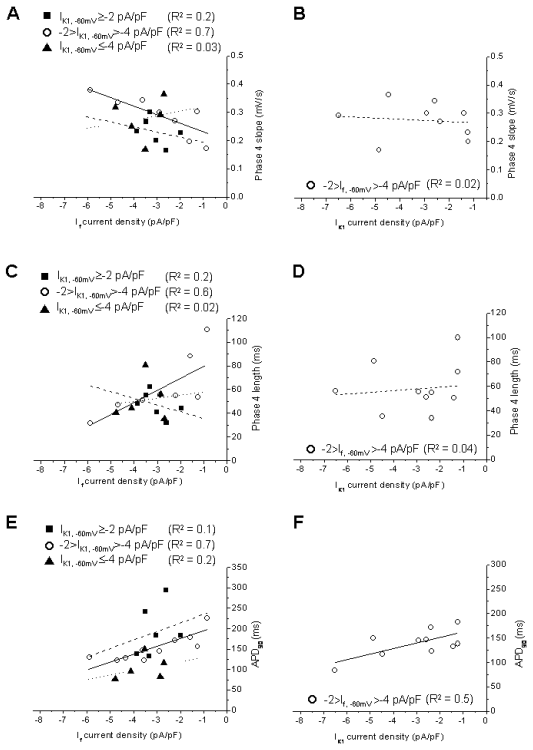

Figure 5.

(A) Correlations between I_f and the phase 4 slope of spontaneously AP-firing cells when $I_{K1, -60mV} \geq -2$ pA/pF (■), $-2 > I_{K1, -60mV} > -4$ pA/pF (○) and $I_{K1, -60mV} \leq -4$ pA/pF (▲). **(B)** Correlations between I_{K1} and the phase 4 slope when $I_{f, -60mV} \geq -2$ pA/pF (■), $-2 > I_{f, -60mV} > -4$ pA/pF (○) and $I_{f, -60mV} \leq -4$ pA/pF (▲). **(C)** Correlations between I_f and the phase 4 length of spontaneously AP-firing cells when $I_{K1, -60mV} \geq -2$ pA/pF (■), $-2 > I_{K1, -60mV} > -4$ pA/pF (○) and $I_{K1, -60mV} \leq -4$ pA/pF (▲). **(D)** Correlations between I_{K1} and the phase 4 length when $I_{f, -60mV} \geq -2$ pA/pF (■), $-2 > I_{f, -60mV} > -4$ pA/pF (○) and $I_{f, -60mV} \leq -4$ pA/pF (▲). **(E)** Correlations between I_f and the APD_{90} of spontaneously AP-firing cells when $I_{K1, -60mV} \geq -2$ pA/pF (■), $-2 > I_{K1, -60mV} > -4$ pA/pF (○) and $I_{K1, -60mV} \leq -4$ pA/pF (▲). **(F)** Correlations between I_{K1} and the APD_{90} when $I_{f, -60mV} \geq -2$ pA/pF (■), $-2 > I_{f, -60mV} > -4$ pA/pF (○) and $I_{f, -60mV} \leq -4$ pA/pF (▲).

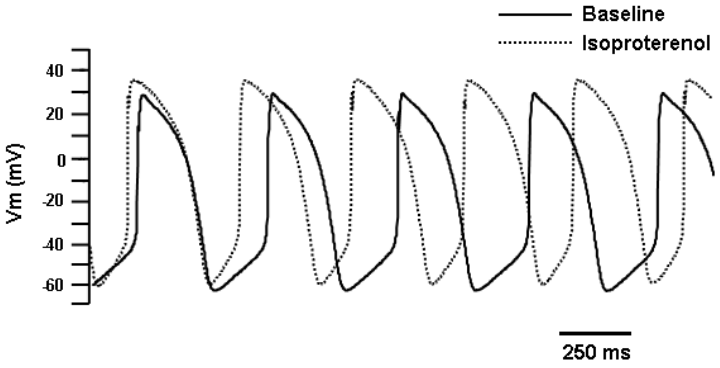

Figure 6.
Effects of adrenergic stimulation by superfusion of 1 μM isoproterenol for 5 minutes (3 cells from a single animal) on HCN1-ΔΔΔ-transduced LV CMs.

Table 1

Summary of AP parameters of control, singly- and co-transduced LV CMs. All values are means ± S.E.

	RMP (mV)	MDP (mV)	APD (ms)	APD_{50} (ms)	APD_{90} (ms)	Phase 4 Length (ms)	Phase 4 Slope (mV/s)	Cycle Length (ms)	Beating Rate (Beats/ min)
Control (17)	-66.0 ± 0.7	--	387.2 ± 10.4	299.5 ± 12.0	357.3 ± 10.0	--	--	--	--
Kir 2.1 (7)	-69.7 ± 0.6	--	138.6 ± 17.6	116.1 ± 17.2	127.8 ± 17.8	--	--	--	--
HCN1-ΔΔΔ (10)	--	-55.8 ± 1.8	207.4 ± 9.4	166.9 ± 6.9	199.5 ± 8.7	88.3 ± 9.6	180.0 ± 20.0	343.7 ± 24.9	181.1 ± 13.1
HCN1-ΔΔΔ + Kir2.1-WT (9)	--	-57.1 ± 1.0	107.37 ± 7.8	72.7 ± 7.8	97.3 ± 7.9	55.0 ± 4.5	280.0 ± 16.0	182.3 ± 6.8	320.0 ± 15.8

n numbers are given in bracket.